Journal of Hazardous Materials 455 (2023) 131648

Contents lists available at ScienceDirect

Journal of Hazardous Materials

journal homepage: www.elsevier.com/locate/jhazmat

Research Paper

Leaching of structural Ca^{2+} ions from a chalcogenide adsorbent by H^+ lifts Cs(I) uptake

Chenyang Yang [a], Yong Jae Suh [b,c,*], Kuk Cho [a,**]

[a] Department of Environmental Engineering, Pusan National University, 2 Busandaehak-ro 63beon-gil, Geumjeong-gu, Busan 46241, Republic of Korea
[b] Resources Utilization Division, Korea Institute of Geoscience and Mineral Resources, 124 Gwahak-ro, Yuseong-gu, Daejeon 34132, Republic of Korea
[c] Department of Resources Engineering, Korea University of Science and Technology, 217 Gajeong-ro, Yuseong-gu, Daejeon 34113, Republic of Korea

HIGHLIGHTS

- A novel KCaSnS adsorbent with metastable Ca^{2+} in Sn-S matrix is designed.
- Cs^+ adsorption capacity amounts to 620 mg/g at pH 2, 68% higher than that at pH 7.
- The enhanced Cs^+ adsorption at pH 2 is due to leaching of structural Ca^{2+} by H^+ and Cs^+.
- The adsorption capacity dependence on pH opposes the general tendency.
- We turn the problematic proton into a functional agent of ion exchange by design.

GRAPHICAL ABSTRACT

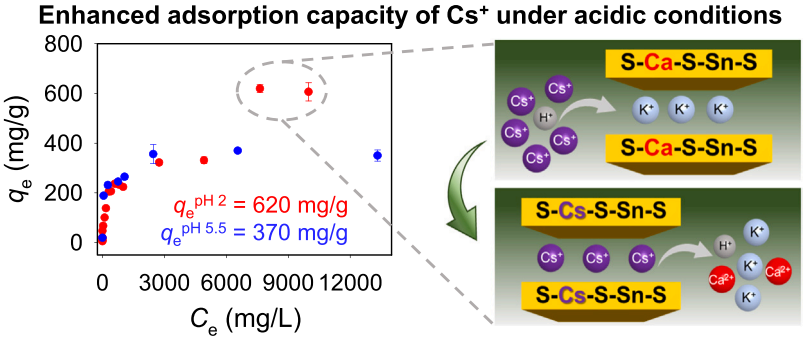

ARTICLE INFO

Editor: Sungjun Bae

Keywords:
Metal sulfide
Caesium
Elution
Proton
Dopant Ca

ABSTRACT

Acidic wastewater containing radioactive ^{137}Cs is difficult to treat by selective adsorption. Abundant H^+ under acidic conditions damages the structure of adsorbents and competes with Cs^+ for adsorption sites. Herein, we designed a novel layered calcium thiostannate (KCaSnS) that contains Ca^{2+} as a dopant. The dopant Ca^{2+} ion is metastable and larger than the ions attempted before. The pristine KCaSnS demonstrated a high Cs^+ adsorption capacity of 620 mg/g at 8250 mg/L Cs^+ solution and pH 2, which is 68% higher than that at pH 5.5 (370 mg/g), a trend opposite to all previous studies. The neutral condition allowed the release of Ca^{2+} present only in the interlayer (~20%); whereas the high acidity facilitated the leaching of Ca^{2+} from the backbone structure (~80%). The complete structural Ca^{2+} leaching was made possible only by a synergistic interaction of highly concentrated H^+ and Cs^+. Doping a large enough ion, such as Ca^{2+}, to accommodate Cs^+ into the Sn-S matrix upon its liberation opens a new way of designing high-performance adsorbents.

* Corresponding author at: Resources Utilization Division, Korea Institute of Geoscience and Mineral Resources, 124 Gwahak-ro, Yuseong-gu, Daejeon 34132, Republic of Korea.
** Corresponding author.
E-mail addresses: aumsuh@kigam.re.kr (Y.J. Suh), kukcho@pusan.ac.kr (K. Cho).

https://doi.org/10.1016/j.jhazmat.2023.131648
Received 13 March 2023; Received in revised form 2 May 2023; Accepted 14 May 2023
Available online 16 May 2023

1. Introduction

Nuclear power, as a relatively clean energy considering air pollutants and CO_2 emissions, has been used to create electricity to meet the world's energy needs. Nonetheless, the growth of the nuclear sector generates environmental and safety problems due to the accumulation of radiotoxic waste. ^{137}Cs is one of the major fission products and is considered a hazardous radioactive element with a half-life of approximately 30 years [19], and ^{137}Cs emits beta-particles and strong gamma-rays in the decay process. It is also easily assimilated into the living body because of its high solubility in water and its similar transport behavior to those of K^+. Thus, Cs^+ removal from radioactive wastewaters has been investigated in many previous studies. It is known that selective removal of Cs^+ from practical nuclear wastewater is difficult owing to interference with high concentrations of coexisting non-radioactive cations [25]. In particular, a high concentration of protons in acidic wastewater inhibits the removal of Cs^+. The radioactive wastewaters generated from reprocessing spent fuel and decommissioning nuclear power plants (NPPs) are usually acidic (pH < 2.3) [12,25]. However, effective and selective Cs^+ removal from acidic radioactive fluids remains a significant difficulty.

Adsorption by ion exchange is a promising wastewater remediation technology for NPPs because of its advantage of treating trace amounts of pollutant with ease [15]. Metal sulfides are considered a remarkable selective class of ion exchangers for Lewis-soft acid treatment because of the presence of Lewis-soft base S^{2-} in their structure. However, most of the existing metal sulfides, such as InSnOS [26], KMS-1 [10], KMPS-1 [18], KMS-2 [11], and KATS-2 [29] showed low adsorption capacity or distribution coefficient for Cs^+ in highly acidic conditions. This is because they have only interlayer cations as ion-exchangeable species. A recent report demonstrated that a structural dopant cation, in addition to interlayer ions, could also contribute to adsorption by being leached out under acidic conditions [30]. However, presumably owing to the significantly smaller size of the dopant cation (Al^{3+}, $r = 0.54$ Å)) than that of Cs^+ ($r = 1.67$ Å) [20], Cs^+ cannot reside in the original Al^{3+} sites, and protons, which are much smaller and abundant, are deposited instead. This presumption suggests that if dopant cations are more comparable in ionic size to Cs^+ and leachable in acid, the dopant lattice positions in the crystal structure of adsorbent can operate as additional active adsorption sites for Cs^+. Metal sulfides doped with an intermediate-sized dopant cation will provide much higher capacity for Cs^+ adsorption in acidic conditions as long as the crystal structure is stable in acid.

Herein, we designed a novel layered metal sulfide, potassium calcium thiostannate (KCaSnS), by introducing Ca^{2+} into the Sn-S matrix, assuming that Ca^{2+} ($r = 1.00$ Å) provides a large enough space for Cs^+ to reside after its release from the lattice structure [20]. Calcium sulfide is readily dissolvable under acidic conditions [2,21], and Ca^{2+} is a much harder Lewis acid than Cs^+. Therefore, we conjectured that the metastable structural Ca^{2+} in addition to the interlayered K^+ will be exchanged for Cs^+ at low pH, possibly resulting in a notable increase in the adsorption capacity. As hypothesized, our experiments demonstrated a high adsorption capacity of 620 mg/g for Cs^+ at pH 2, the highest value to date. Even though the result was obtained at very high Cs^+ concentration, which is not in a practical situation, this approach is original in its design of novel chalcogenide adsorbents for highly acidic wastewater treatment.

2. Methods

The information of chemicals and characterization techniques can be accessed in Sections S1 and S2 of Supporting Information. Equations used for data analysis and their corresponding descriptions can be found in Sections S3 and S4.

2.1. Hydrothermal synthesis of KCaSnS

A new KCaSnS adsorbent was synthesized by a hydrothermal method as follows: Briefly, the chemicals, potassium carbonate (K_2CO_3, 24 mmol), calcium chloride dihydrate ($CaCl_2{\cdot}2\ H_2O$, 6 mmol), tin powder (Sn, 24 mmol), sulfur (S, 120 mmol), and about 2 mL of deionized water, were mixed in an agate mortar. The mixture was transferred into a 100 mL Teflon-lined autoclave and heated in a furnace at 200 ℃ for 24 h. After cooling the autoclave to room temperature, the resultant powder was collected by centrifugation. Then, the powder was washed with acetone and deionized water, and dried in a vacuum oven at 60 ℃ for 18 h.

2.2. Ion exchange experiments

Considering the hazard of ^{137}Cs, all experiments in this study were performed using its nonradioactive isotope. A typical experiment was conducted in a 30 mL glass vial containing 25 mL Cs^+ solution and 25 mg of KCaSnS (solid/liquid ratio, S/L = 1 g/L) at room temperature in three batches. The solid-liquid mixture was shaken in a shaker for a certain period, and the solid was separated with a 0.22 μm PVDF filter. The filtrate was then diluted and analyzed for Cs^+ concentration using an atomic absorption spectrometer. The solid residuals after adsorption under acidic and neutral conditions were named as Cs-KCaSnS-acidic and Cs-KCaSnS-neutral, respectively. Furthermore, for ease of description, the pH range of 5–9 is signified as a neutral condition. When the pH of a solution is less than 3, it is said to be acidic.

In kinetics studies, KCaSnS powder was mixed with approximately 20 and 1000 mg/L Cs^+ solutions of pH 2 and 7 for various times of 1, 5, 15, 30, 60, 120, 300, and 1080 min. The isotherm experiments were conducted under neutral and acidic conditions with various Cs^+ concentrations (5.00–10600 mg/L at pH ~2; 19.1–13700 mg/L at pH ~5.5).

To study the effect of pH on the performance of KCaSnS for Cs^+ adsorption, approximately 20 mg/L of Cs^+ solutions with a pH range of 1–13 were prepared by adjusting pH with HCl and NaOH solutions. The adsorption performance of KCaSnS toward Cs^+ under acidic conditions was further investigated by dissolving the required amounts of $NaNO_3$, KNO_3, $Mg(NO_3)_2{\cdot}6\ H_2O$, and $Ca(NO_3)_2{\cdot}4\ H_2O$ in Cs^+ solution (~20 mg/L). Besides, the ion exchange performance of KCaSnS in real water environments was evaluated using ~20 mg/L Cs^+ spiked artificial seawater (ASW) and tap water (TW) (Busan, Korea) with a natural pH (7.8 for ASW; 7.4 for TW) and pH 2. The contact time was set to 5 h.

The reusability of KCaSnS under acidic conditions was investigated by a series of adsorption and desorption tests. In the adsorption process, a mixture of 500 mg KCaSnS and 500 mL of 1000 mg/L Cs^+ solution with a pH ~2 was kept on a shaker for 5 h. Then, the adsorbed Cs ions were eluted from Cs-KCaSnS-acidic with each 500 mL of 1 M KCl solution, 1 M $CaCl_2{\cdot}2\ H_2O$ solution, and a mixture of 1 M KCl and 1 M $CaCl_2{\cdot}2\ H_2O$, respectively. The resulting products are named KCaSnS-K, KCaSnS-Ca, and KCaSnS-K&Ca, respectively. In addition, a two-step elution test was run using a 1 M $CaCl_2{\cdot}2\ H_2O$ and a 1 M KCl solution in sequence, whose product is named KCaSnS-Ca-K. All of the particles produced were rinsed several times with deionized water before being employed in subsequent Cs^+ adsorption studies.

3. Results

3.1. Characteristics of KCaSnS

Important properties of the as-synthesized KCaSnS, such as morphology, elemental distribution and composition, crystalline phase, and electron binding energy, were analyzed using various techniques. A field-emission scanning electron microscopy (FE-SEM) image of the pristine KCaSnS exhibited a plate-like morphology (Fig. 1a), and elemental mapping analysis showed a uniform distribution of K, Ca, Sn,

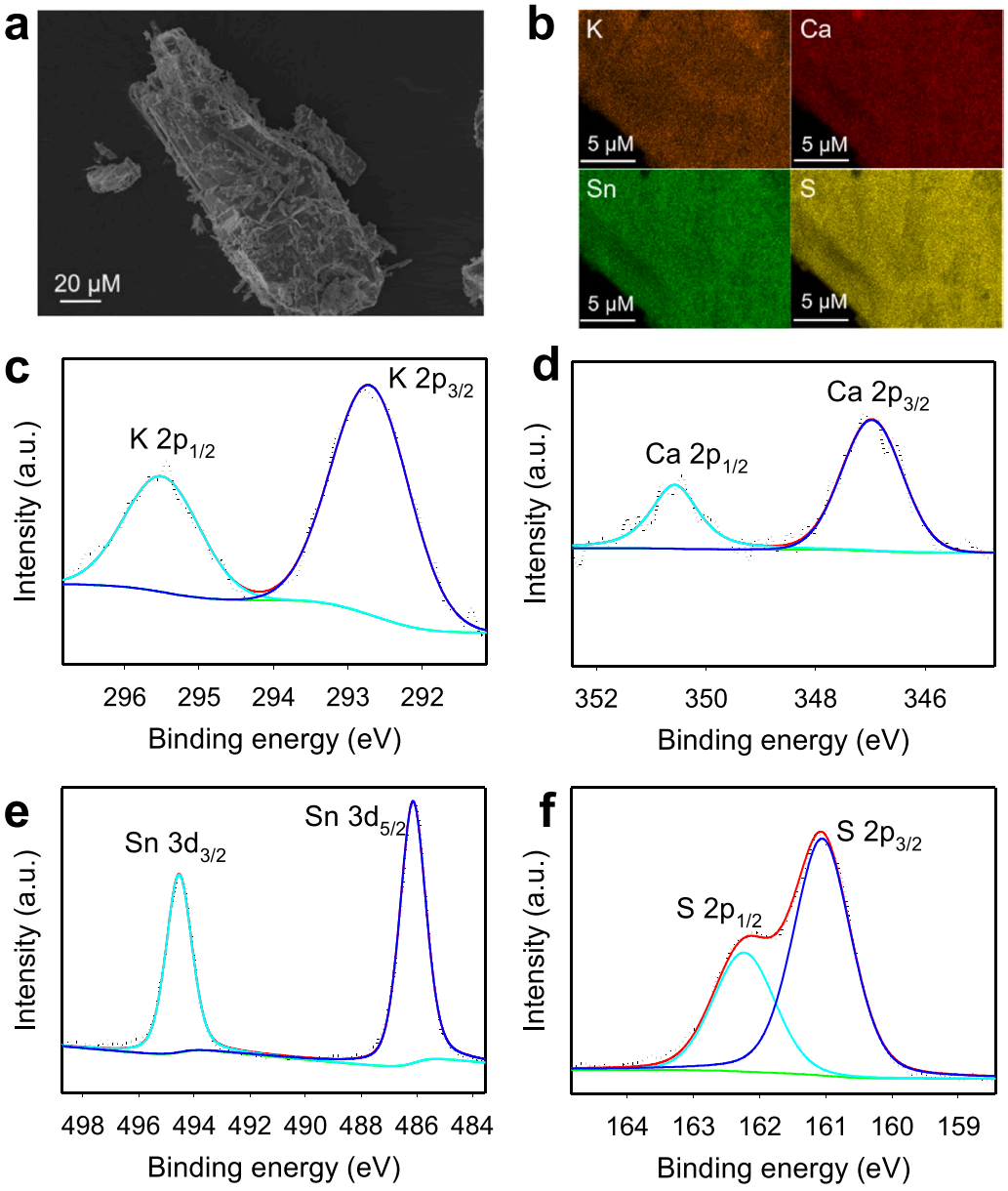

Fig. 1. Morphology, elemental distribution, and XPS spectra of the pristine KCaSnS. **a** FE-SEM image and **b** elemental mapping. High-resolution XPS spectra of **c** potassium, **d** calcium, **e** tin, and **f** sulfur.

and S in KCaSnS (Fig. 1b). Energy dispersive X-ray spectroscopy (EDS) showed the stoichiometry of $K_{1.49}Ca_{0.81}Sn_3S_{6.08}$ (Table S1); the more accurate composition analyzed using inductively coupled plasma-optical emission spectrometry (ICP-OES) was $K_{1.35}Ca_{0.91}Sn_3S_{7.59}$. X-ray photoelectron spectroscopy (XPS) spectra (Fig. 1c–f) revealed the characteristic peaks of K (292.7 and 295.5 eV), Ca (347.0 and 350.6 eV), Sn (486.1 and 494.5 eV), and S (161.1 and 162.2 eV) [13]. The stability of the pristine KCaSnS was investigated at various pH values. From pH 4–12, the samples retained their original crystal structure (Fig. S1). However, a new Bragg peak at 15.0° appeared at pH 2, and the characteristic peaks of $CaSn(OH)_6$ appeared at pH 13 because of the high concentrations of proton and hydroxide ions at the respective pHs.

3.2. Kinetics of Cs^+ adsorption

The adsorption kinetics was studied to know how fast the Cs^+ adsorption takes place. Fig. 2 shows that KCaSnS displayed quick adsorption kinetics in both neutral and acidic environments with an initial concentration of ~20 mg/L. Cs^+ concentration achieved equilibrium in the first minute under neutral circumstances (Fig. 2a), showing a steep decrease in concentration from 20 to 0.136 mg/L. This indicates a removal efficiency of 99.3% in 1 min, which is higher than that of KTS-3 ($K_{1.92}Sn_{3.04}S_{7.04}$: 94% in 5 min) [19], SbS-1 K ($K_2Sb_4S_7{\cdot}2\ H_2O$: 93% in 2 min) [33], AgSnSe-1 ($[NH_3CH_3]_{0.5}[NH_2(CH_3)_2]_{0.25}Ag_{1.25}SnSe_3$: 88% in 4 h) [3], FJSM-4 ($[(EtNH_3)_{1.68}(Et_2NH_2)_{0.32}]Sn_3S_7{\cdot}0.68\ H_2O$: 79% in 30 min) [7], and NVPC ($(NH_4)_2[(VO)_2(HPO_4)_2C_2O_4]{\cdot}5\ H_2O$: 52% in 1 min) [34].

Under acidic conditions, slow kinetics has generally been observed for the adsorption of Cs^+ because of severe competition with protons. Notably, KCaSnS exhibited fast adsorption kinetics at pH 2. As shown in Fig. 2b, the Cs^+ adsorption reached equilibrium within 1 min, with a removal efficiency of 95.4%, which is substantially faster than that of FJSM-4 (78% in 5 min) [7], and DB-ZrP (3,4-dibenzo-21-crown-7 intercalated zirconium phosphonate: 70% in 60 min) [14]. It is worth noting that the adsorption of Cs^+ can still reach equilibrium within 30 min with a high initial concentration of ~1000 mg/L under both

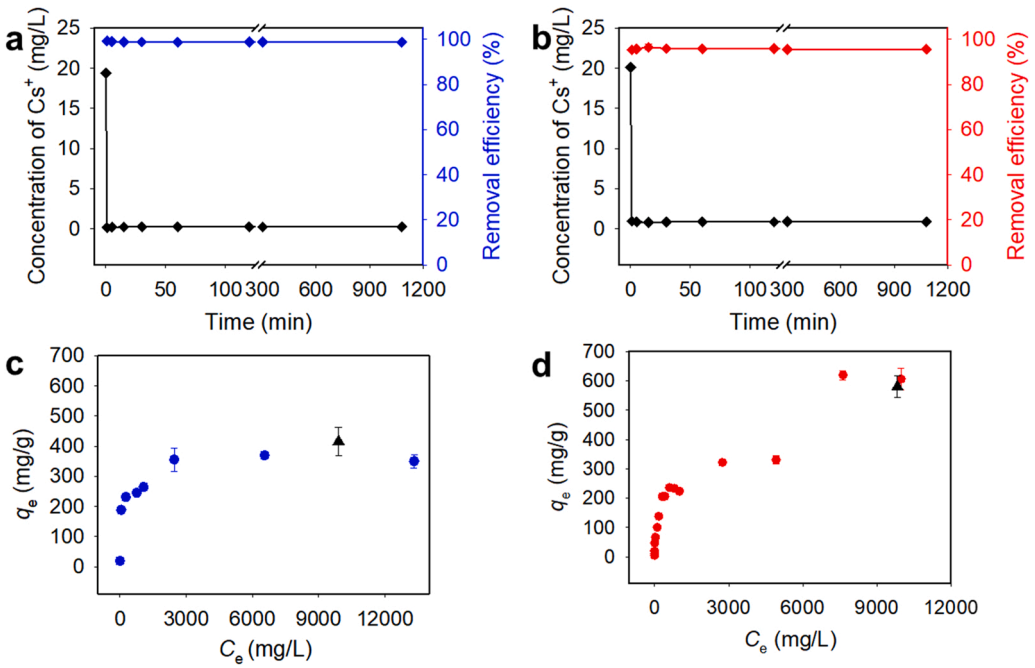

Fig. 2. Kinetics curves of KCaSnS at **a** neutral condition and **b** pH 2 (C_0^{Cs} = ~20 mg/L); Equilibrium data for Cs^+ adsorption by KCaSnS at **c** neutral condition and **d** pH 2. The symbol ▲ in the plots **c** and **d** represents the adsorption result for the adsorbent that was first allowed to reach equilibrium at 10000 mg/L Cs^+ and pH 2 and then regenerated with KCl solution.

neutral and acidic conditions (Fig. S2 and Table S2).

3.3. Cs^+ adsorption isotherm

To investigate the maximum Cs^+ adsorption capacities of KCaSnS under neutral and acidic conditions, the isotherm study was conducted using low to extremely high concentrations of Cs^+ solutions. Under neutral conditions, equilibrium adsorption capacity (q_e, mg/g) rapidly increased with the equilibrium concentration of Cs^+ in solution (C_e, mg/L) up to 370 mg/g or 2.78 mmol/g (Fig. 2c). The q_e value is lower than ~460.8 mg/g for hf-TiFC (hollow flower-like titanium ferrocyanide) [31], 453 mg/g for MIL-101-SO_3H [1], 437.5 mg/g for NVPC [34], and 400 mg/g for FJSM-SnS-4 [7]. But it is higher than that of most other adsorbents, such as ~252.1 mg/g for $NH_4V_4O_{10}$ (layered ammonium vanadate) [32], 250.3 mg/g for KAlSnS-3 ($K_{1.83}Al_{0.48}Sn_3S_{7.64}$) [30], ~222 mg/g for KMS-1 ($K_{1.9}Mn_{0.95}Sn_{2.05}S_6$) [10], and 174 mg/g for AgSnSe-1 [3], and much higher than ~82.7 mg/g for commercial AMP-PAN (ammonium molybdophosphate–polyacrylonitrile) [16] (Fig. 3a).

In acidic solutions, KCaSnS showed a significantly enhanced adsorption capacity toward Cs^+. Unlike at neutral conditions, q_e increased stepwise with C_e in acidic solutions (Fig. 2d). The sites, which proton would occupy, appeared to be adsorbed by Lewis softer Cs^+ above the Cs^+ concentration of 8250 mg/L. The saturated adsorption capacity was as high as 620 mg/g, or 4.66 mmol/g, which is the highest value among those measured at a pH value near 2.0. The other adsorbents with high capacities include KAlSnS-3 (170 mg/g at pH 2) [30], KMS-1 (168 mg/g at pH 2.5) [10], and DB-ZrP (155.42 mg/g at pH 1) [14]. KCaSnS has a substantially greater adsorption capacity at pH 2 than FJSM-SnS-4 (144.8 mg/g at pH 1.6) [7] and NVPC (65 mg/g at pH 2.05) [34], which have higher adsorption capacities than KCaSnS in neutral conditions (Fig. 3a). Although the maximum capacity of KCaSnS at pH 2 appeared to be unrealistically high, a low standard deviation range of all the equilibrium data shown in both Fig. 2c and 2d proved accuracy of the results. The detailed explanation of this peculiar trend will be provided in Discussion later.

3.4. pH-dependent Cs^+ adsorption

To further investigate the influence of solution acidity or basicity on the Cs^+ adsorption, adsorption experiments were performed over the pH range of 1–13. As shown in Fig. 4a, more than 97.8% of Cs^+ was

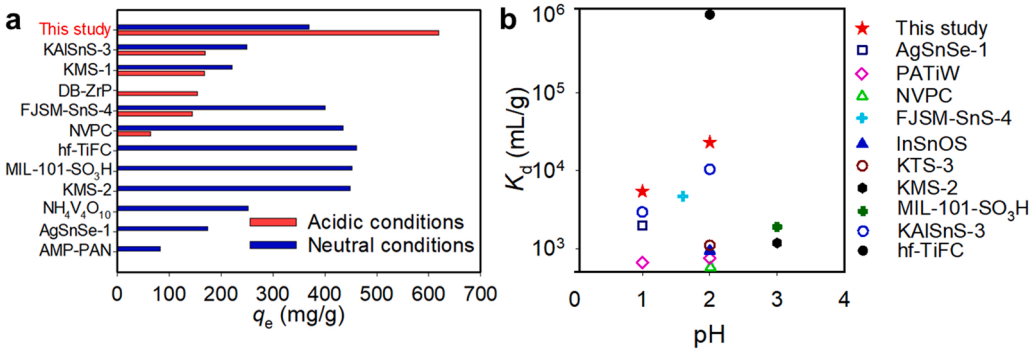

Fig. 3. Comparison of **a** adsorption capacity (q_e) and **b** distribution coefficient (K_d) of representative adsorbents. pH values for acidic conditions of q_e ranges from 1 to 3. q_e of some adsorbents were obtained from the corresponding figures of the references using GetData Graph Digitizer.

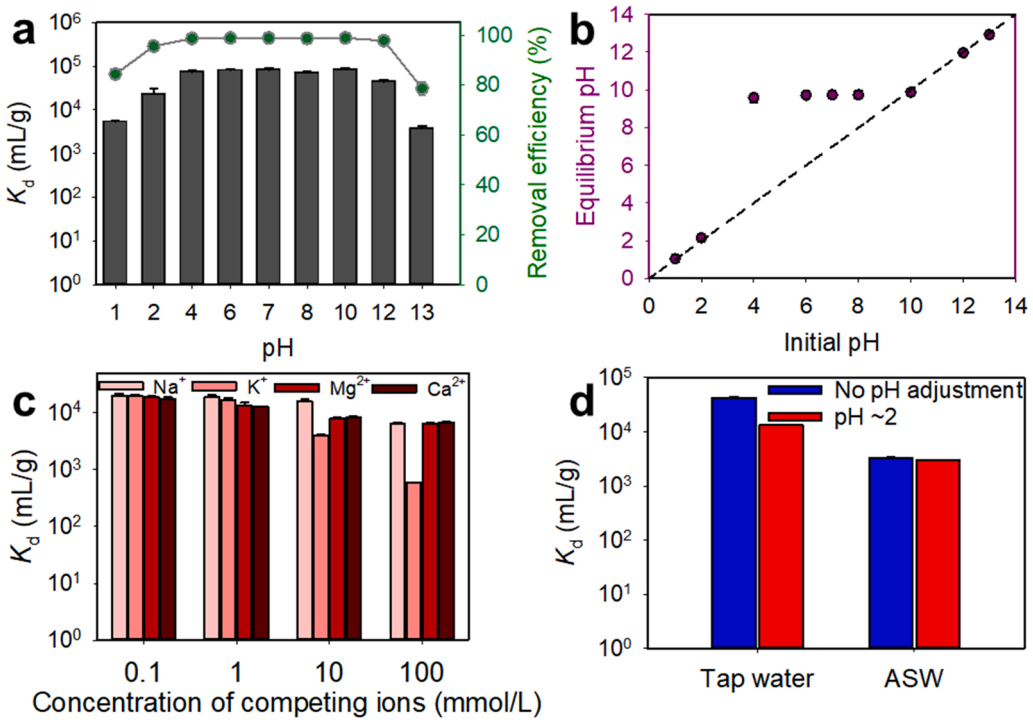

Fig. 4. **a** K_d and removal efficiency of KCaSnS at different pH conditions; **b** equilibrium pH values after Cs^+ adsorption at various initial pH values; **c** variation in K_d for Cs^+ at various concentrations of competing ions (pH: ~2); **d** selective removal of Cs^+ by KCaSnS in natural and acid-spiked water systems. C_0^{Cs} = ~20 mg/L.

removed in the pH range of 4–12, and the distribution coefficient (K_d) was higher than 4.39×10^4 mL/g. On the other hand, at pH 13, K_d slightly decreased to 3.72×10^3 mL/g. The decrease in K_d might be due to the partial decomposition of KCaSnS to $CaSn(OH)_6$; whereas the pristine crystal structure was preserved in the pH range of 4–12 (Fig. S1). Meanwhile, at the initial pH range of 4–8, the adsorption experiments resulted in an increase in the final solution pH, implying competitive adsorption of protons in the lower Cs^+ concentrations at the end stage (Fig. 4a and 4b) [9]. Despite the competition between Cs^+ and protons, the K_d values at pH 1 and 2 were as high as 5.41×10^3 mL/g and 2.30×10^4 mL/g, respectively. In acidic solutions, KCaSnS shows higher values of K_d than AgSnSe-1 [3], KAlSnS-3 [30], InSnOS ($(Heta)_{9.5}(H_3O)_{2.5}[In_8Sn_{12}O_{10}S_{32}]\cdot 22\ H_2O$) [26], KTS-3 [19], KMS-2 [11], and PATiW (polyaniline titanotungstate) [4], except for hf-TiFC [31] (Fig. 3b). It is worth noting that the K_d of KCaSnS under acidic conditions is also higher than that of FJSM-SnS-4 [7], NVPC [34], and MIL-101-SO_3H [1], all of which have higher adsorption capacities than KCaSnS in neutral conditions.

3.5. Effect of interfering ions on the Cs^+ adsorption in different water systems

High concentrations of nonradioactive ions such as Na^+, K^+, Mg^{2+}, and Ca^{2+} in the radioactive wastewater inhibit the selective adsorption of Cs^+. Furthermore, protons contained in radioactive wastewaters created during NPP decommissioning and spent fuel reprocessing interfere with Cs^+ adsorption via two routes: the breakdown of the adsorbent structure and the competition for adsorptive sites with Cs^+. Accordingly, the adsorption performance of KCaSnS in acidic solutions with various concentrations of competing ions was investigated. As shown in Fig. 4c, when the concentrations of competing ions ranged from 0.1 to 1 mmol/L, the K_d for Cs^+ was higher than 1.27×10^4 mL/g. The effects of divalent Mg^{2+} and Ca^{2+} were more prominent than those of monovalent Na^+ and K^+ in this range because of stronger electrostatic interaction at a relatively low ionic strength [6].

In contrast, the interference of K^+ in the adsorption of Cs^+ was more significant at concentrations from 10 to 100 mmol/L. Because the electric double layer is compressed in a high ionic strength solution, chemical hardness or affinity takes precedence in ion exchange [23]. As Lewis soft base S^{2-} has higher affinity for the relatively soft acids Cs^+ (chemical hardness $\eta = 9.63$ eV) and K^+ ($\eta = 13.64$ eV) than for the hard acids Na^+ ($\eta = 21.07$ eV), Mg^{2+} ($\eta = 32.55$ eV), and Ca^{2+} ($\eta = 19.52$ eV) [8,17], KCaSnS showed stable adsorption performance toward Cs^+ in the presence of Lewis hard competing ions except for K^+ at a high ionic strength.

To simulate a more practical case, the adsorption performance of KCaSnS toward Cs^+ was investigated in different water environments, including TW, ASW, and acid-spiked TW and ASW. The main components in each solution are listed in Table S3. KCaSnS showed high distribution coefficients for Cs^+ in TW (4.30×10^4 mL/g) and ASW (3.29×10^3 mL/g) (Fig. 4d). Notably, the high K_d values can be maintained even in the acid-spiked water systems, i.e., 1.33×10^4 mL/g in acidic TW and 2.95×10^3 mL/g in acidic ASW. The values of K_d in neutral conditions are comparable to previous works such as KAlSnS-3 [30] and SbS-1 K [33] (Table S4). One might consider the acidic TW and ASW impractical; in this study, they are just simulated acidic water based on real water resources.

3.6. Reusability of KCaSnS

To study the behavior of the structural Ca^{2+} on the recyclability of KCaSnS under acidic conditions, we conducted a series of adsorption-desorption experiments using different eluents. When Ca^{2+} was used as an eluent, some Cs^+ remained in the structure (Table S6) because Cs^+ is chemically softer than Ca^{2+}. This resulted in a lower adsorption capacity of KCaSnS-Ca than that of the pristine KCaSnS (Fig. 5a). With K^+ as an eluent, most of the Cs^+ in both the interlayer and structure were replaced with K^+ (Table S6) because K^+ has similar chemical hardness and ionic radius ($r = 1.38$ Å) to Cs^+ ($r = 1.67$ Å). As the concentration of K^+ is rather high (1 mol/L), some structural Ca^{2+} ions might be further replaced with K^+. In the successive adsorption test, the replaced K^+ was readily exchangeable with Cs^+ at high Cs^+ concentrations,

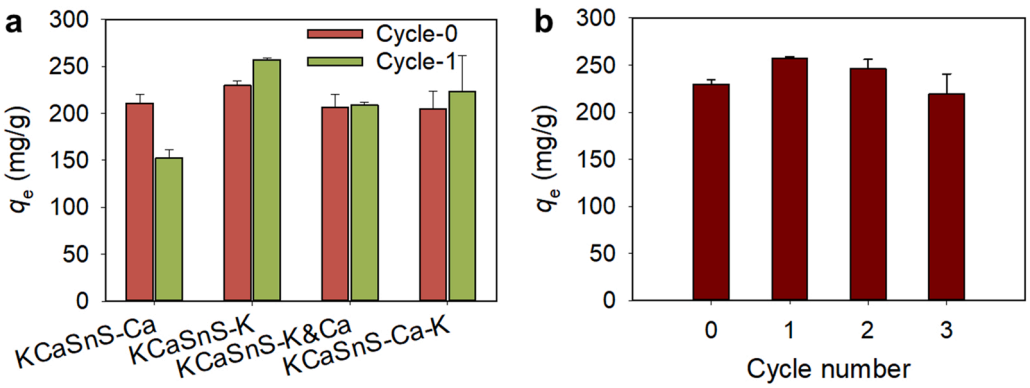

Fig. 5. Adsorption capacity q_e of the pristine KCaSnS and the adsorbents regenerated **a** using different eluents in one cycle of adsorption-desorption and **b** using an eluent KCl, in three successive cycles of adsorption-desorption. $C_0^{Cs} = \sim$1000 mg/L and pH 2.

resulting in higher adsorption capacity (Fig. 5a). For the eluent containing both K^+ and Ca^{2+}, most of the structural Ca^{2+} in the Cs-KCaSnS-acidic might remain in the structure because of the high concentration of Ca^{2+} in the solution. As K^+ replaced most of the adsorbed Cs^+ (Table S6), the adsorption capacity of KCaSnS-K&Ca was similar to that of pristine KCaSnS (Fig. 5a). Finally, the two-step elution with Ca^{2+} and K^+ in succession produced a product with approximately the same elemental composition as the regenerated KCaSnS-K. (Table S6). This indicated that the intermediate regeneration step with Ca^{2+} did not influence the second K^+ regeneration step. Thus, KCaSnS-Ca-K showed the same trend of an increase in the adsorption capacity as KCaSnS-K (Fig. 5a).

To further evaluate the reusability, regeneration tests with an eluent solution of KCl were performed three times successively. The first, second, and third regenerated adsorbents were named KCaSnS-K-1, KCaSnS-K-2, and KCaSnS-K-3, respectively. As mentioned earlier, KCaSnS-K-1 showed a higher adsorption capacity than the pristine KCaSnS; whereas the capacity gradually decreased in the second and third regeneration tests, finally reaching that of the pristine KCaSnS (Fig. 5b). The reason for the capacity reduction might be attributed to the remaining K during adsorption. The XRD patterns of the second (KCaSnS-K-2) and third (KCaSnS-K-3) regenerated samples showed two distinct peaks at 9.9° and 11.9° instead of the doublet that existed in that of the first regenerated adsorbent (KCaSnS-K-1) (Fig. S4a). The right shift of the peak indicates that the interlayer spacing was narrowed in the second and third regenerated samples, implying more remaining K along with the regeneration. In summary, the clear crystallinity of the regenerated adsorbents indicates that KCaSnS is highly reusable in acidic conditions.

4. Discussion

We have provided the major data on the Cs^+ adsorption of a newly developed tin sulfide, KCaSnS, thus far. Because the experimental results revealed complicated behaviors caused by interactions between the various ions in the aqueous solution and the adsorbent, a thorough explanation incorporating all relevant data and hypotheses may be necessary. Accordingly, the Cs^+ adsorption mechanism and the behavior of Ca^{2+} upon adsorption will be discussed in detail in the following, along with the concluding remarks on design strategy.

4.1. Cs^+ removal mechanism

The removal of Cs^+ was found to occur via the ion exchange mechanism under both neutral and acidic conditions by SEM-EDS, ICP-OES, X-ray diffraction (XRD), and XPS analyses. In the adsorption experiments under neutral conditions, the plate-like morphology of KCaSnS was preserved after adsorption (Fig. S3a). Fig. 6 shows high-resolution XPS spectra with the typical peaks of Cs 3d appearing while the clear peaks of K 2p vanished and the intensity of Ca 2p dropped, showing ion exchange between K^+/Ca^{2+} and Cs^+. The same ion exchange behavior was semi-quantitatively revealed in the EDS analysis of Cs-KCaSnS-neutral: the amount of K and Ca decreased while the amount of Cs increased in comparison with the pristine KCaSnS (Table S1). Furthermore, more precise data obtained using ICP-OES analysis revealed the composition change with a charge ratio of 0.826 for the adsorbed Cs^+ to the released cations (K^+ and Ca^{2+}) (Table S5), suggesting the ion exchange process in neutral conditions.

Under acidic conditions, the adsorption experiments revealed the ion exchange between K^+/Ca^{2+} in the adsorptive sites and the adsorbates Cs^+/H^+. The EDS results showed a decrease in the amount of K and Ca and an increase in the amount of Cs in Cs-KCaSnS-acidic (Table S1). Without conversion of the KCaSnS morphology (Fig. S3b), the trend of changes in the XPS spectra of Cs, K, and Ca upon adsorption under the acidic conditions were the same as that in the neutral conditions (Fig. 6). Notably, the intensity of Ca 2p almost disappeared in Cs-KCaSnS-acidic (Fig. 6c), indicating the removal of most Ca from KCaSnS. The additional Ca leaching from the adsorbent is attributed to the presence of abundant protons in the acidic solutions. The role of protons in leaching Ca was confirmed by a separate experiment using a Cs-free acidic solution with pH 2. According to the ICP-OES analysis (Table S5), the charge ratio of the reduced H^+ to the sum of the released K^+ and Ca^{2+} was 1.01, indicating the adsorption of H^+ even onto the structural sites of Ca^{2+}. In the presence of Cs^+, the released adsorptive sites might be occupied by both H^+ and Cs^+. The changes in the composition of the Cs^+ solutions obtained by ICP-OES revealed that the charge ratio of the sum of the adsorbed Cs^+ and H^+ to the sum of the released K^+ and Ca^{2+} was 0.853, substantially greater than 0.368 when just Cs^+ was regarded as an adsorbate (Table S5). As the solution pH was increased from 2.05 to 2.14 after the experiment, the loss of H^+ in the solution was assumed to be adsorbed by the adsorbent. The proton appeared to be less competitive for adsorption than Cs^+ as the molar ratio of H^+ to Cs^+ was 2.56 and 1.32 in the feed solution and in Cs-KCaSnS-acidic, respectively. Therefore, the Cs^+ removal mechanisms in both the neutral and acidic conditions were the ion exchange between the cations present in the system except for Sn^{4+}.

4.2. Identification of Ca^{2+} location in KCaSnS

The Ca^{2+} ions in the pristine KCaSnS were found to be present in both the interlayer and crystalline structures. In the neutral pH, CaS bond in KCaSnS is stable, and thus Ca^{2+} present only in the interlayer might be released into the aqueous solution. The release of the interlayered Ca^{2+} was evidenced by a decrease in Ca from 0.81 to 0.11 mol in the semi-quantitative EDS data (Table S1), indicating partial release. To confirm our hypothesis further, Ca^{2+} leaching tests were conducted using different concentrations of $CsNO_3$ solutions in neutral conditions.

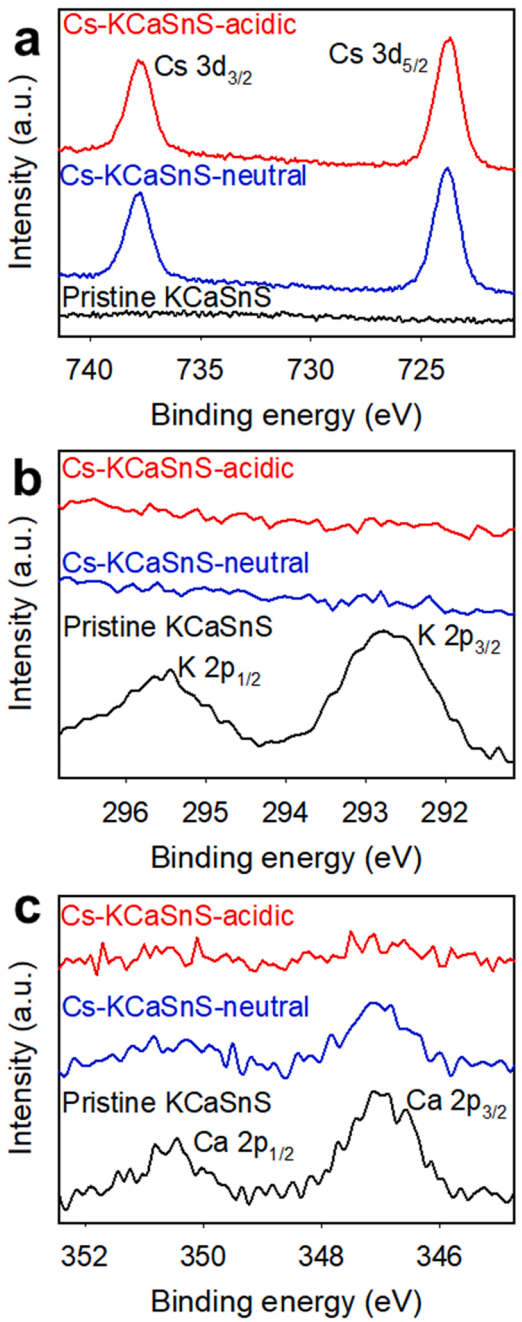

Fig. 6. High-resolution XPS spectra of **a** Cs, **b** K, and **c** Ca in KCaSnS, Cs-KCaSnS-neutral, and Cs-KCaSnS-acidic, respectively.

Over the initial Cs^+ concentration range of 3.78–101 mmol/L, the amount of Ca^{2+} leached out was kept nearly constant at about 20% (Section S4 and Fig. 7a). Besides, the XRD pattern indicated that the ion exchange is topotactic (Fig. S4b). The peak near 10° in the XRD pattern corresponded to the interlayer space of metal sulfides [19,30]. The enlarged XRD pattern of the pristine KCaSnS (Fig. S5) revealed two peaks at 10°, which are attributable to the intercalation of Ca^{2+} and K^+ [22,27].

Given the Ca^{2+}-leaching-test results above, the structural Ca^{2+} might amount to about 80%. The incorporation of Ca^{2+} into the Sn-S crystal structure was substantiated by XPS analysis. As shown in Fig. 1f, the binding energy of S $2p_{3/2}$ (161.05 eV) in the pristine KCaSnS was lower than that in KTS-3 (161.5 eV) [19] and KAlSnS-3 (161.28 eV) [30]. The electron binding energy is inversely related to the electron density around an atom [28]. The electronegativity of Ca ($\chi = 1.00$ by Pauling scale) is lower than that of Al ($\chi = 1.61$) and Sn ($\chi = 1.96$) but higher than that of K ($\chi = 0.82$). If all the Ca^{2+} ions are located only in the interlayer by replacing some interlayered K^+, the binding energy of S $2p_{3/2}$ in KCaSnS should be higher than that in KTS-3, which contradicts the XPS analysis results. The substitution of Ca^{2+} for Al^{3+} in KAlSnS-3 may also reduce the binding energy of sulfur. As a result, the decreased binding energy of S $2p_{3/2}$ in KCaSnS can be ascribed to the effective integration of Ca^{2+} into the Sn-S matrix via Sn^{4+} ion replacement.

4.3. Ca^{2+} leaching enhanced the adsorption of Cs^+

The adsorption capacity of KCaSnS was shown to be higher in the acidic condition than in the neutral condition (Fig. 2c and 2d), which opposes the common behavior of most adsorbents. In the neutral condition, the molar ratio of the adsorbed Cs^+ to the released K^+ was 1.11 (Fig. S6 and Table S5), indicating that the interlayered Ca^{2+} also participated in the ion exchange. Clearly, this molar ratio value is greater than that of prior research in which only K^+ may operate as an exchangeable ion [11,19,29,30]. The portion of the interlayered Ca^{2+} was estimated to be 22.5% (0.30 mmol/L) of the total Ca amount (1.32 mmol/L) in the pristine KCaSnS (Section S4 and Table S5). Given the formula of $K_{1.35}Ca_{0.91}Sn_3S_{7.59}$, complete release of Ca^{2+} in a solid-liquid system of 1 g/L will result in 1.32 mmol/L Ca^{2+} in the filtrate (Section S4). According to the XPS analysis (Fig. 7c), the S 2p binding energy of KCaSnS was reduced by 0.19 eV (from 161.05 to 160.86 eV) after the Cs^+ adsorption, which is greater than that of KAlSnS-3 (0.03 eV) [30] and KATS-2 (0.09 eV) [29] with only K^+ as an exchangeable ion. This can be attributed to the exchange of more electronegative Ca ($\chi = 1.00$) for less electronegative Cs ($\chi = 0.79$) and K ($\chi = 0.82$). Notably, the highest q_e of 370 mg/g (2.78 mmol/g) under neutral conditions was similar to the theoretical adsorption capacity (340 mg/g or 2.56 mmol/g) calculated from the sum of all K^+ and interlayered Ca^{2+} in the pristine $K_{1.35}Ca_{0.91}Sn_3S_{7.59}$ (Fig. 2c). Therefore, we concluded that the interlayered Ca^{2+} in addition to K^+ was replaced with Cs^+ under neutral conditions.

The acidic condition enhanced the Cs^+ adsorption by facilitating the leaching of the structural Ca^{2+}. The Cs^+-free solution with pH 2 leached out 37.1% (0.49 mmol/L) of Ca^{2+}; whereas the Cs^+-rich solution with pH 2 leached out 76.7% (1.01 mmol/L) of Ca^{2+} at $C_0^{Cs} = \sim 500$ mg/L or 3.76 mmol/L (Table S5). They were both higher than in the neutral condition (22.5%). Upon the Cs^+ adsorption, the higher chemical affinity of S for softer Cs^+ than Ca^{2+} and H^+ might further increase the leaching amount of Ca^{2+}. As the charge ratio of the sum of the adsorbed Cs^+ and H^+ to the released K^+ was much higher than unity (1.80) (Table S5), the released Ca^{2+} should have participated in the Cs^+ adsorption. Although H^+ was adsorbed more than Cs^+, probably owing to its higher concentration of 10 mmol/L (pH 2), the molar ratio of the adsorbed Cs^+ to the adsorbed H^+ in this study was 46% higher than that of KAlSnS-3. In KAlSnS-3, Cs^+ cannot be in the structural positions of Al^{3+} because Cs^+ ion ($r = 1.67$ Å) is much larger than Al^{3+} ion ($r = 0.54$ Å). The binding energy of S 2p increased slightly after Cs^+ adsorption in the acidic state, from 161.05 eV to 161.07 eV (Fig. 7d); in the neutral condition, it decreased as previously described (Fig. 7c). This is because the amount of the adsorbed H^+ was higher than that of Cs^+, and H^+ ($\chi = 2.20$) is more electronegative than Cs^+ ($\chi = 0.79$). Nevertheless, this value in Cs-KCaSnS-acidic was lower than that in Cs-loaded KAlSnS-3 at pH 2 (161.30 eV), in which less amount of Cs^+ was adsorbed.

A sharp increase in the Cs^+ adsorption with increasing the initial Cs^+ concentration at pH 2 was corroborated by the XRD analysis (Fig. 7b). In a 500 mg/L Cs^+ case, the Bragg peaks around 10° was right shifted, implying that H^+ was adsorbed more than Cs^+ as agreed with the elemental data. The broadened Bragg peaks indicated a decrease in crystal size and an increase in lattice disorder due to the dominant adsorption of smaller-sized H^+ [5]. As the Cs^+ concentration increased

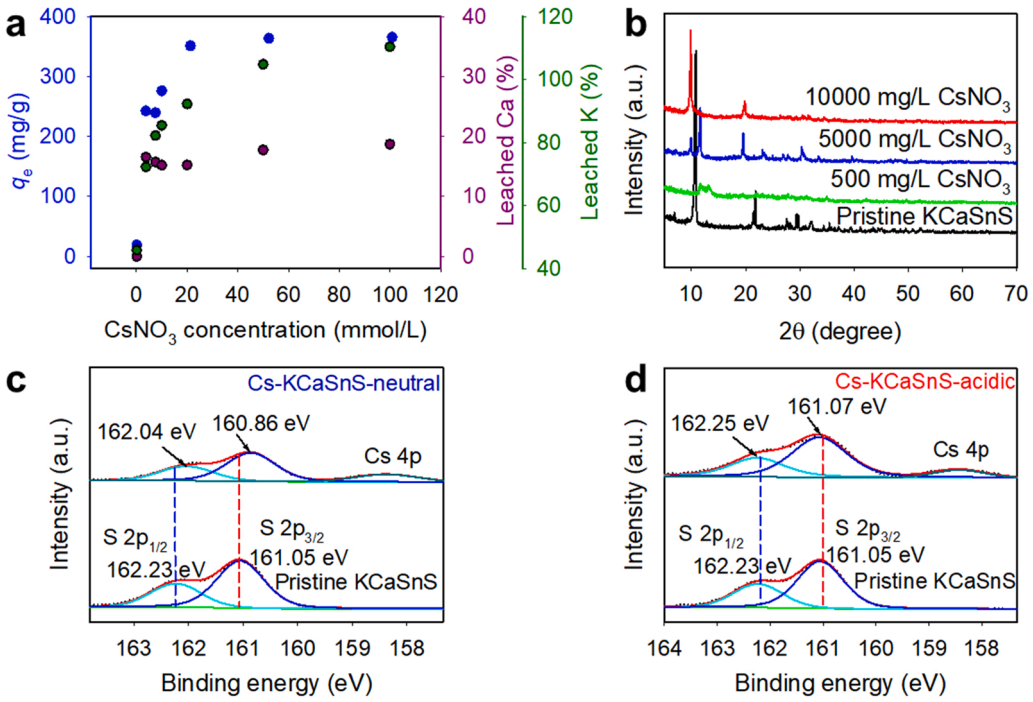

Fig. 7. **a** Ca^{2+} leaching test at different $CsNO_3$ concentrations under the neutral condition; **b** XRD patterns of Cs-loaded KCaSnS after adsorption at different Cs^+ initial concentrations at pH 2, and XPS spectra of sulfur in **c** pristine KCaSnS and Cs-KCaSnS-neutral, and in **d** pristine KCaSnS and Cs-KCaSnS-acidic.

to ~5000 mg/L, the two peaks representing the interlayer spacing were separated more widely than that of the pristine KCaSnS (Fig. 7b and S5). This is attributable to more Cs^+ being adsorbed and the larger ionic-size difference between Cs^+ and H^+. In contrast, in the case of a ~10000 mg/L Cs^+ solution, only a single peak was observed at a lower 2θ position, indicating that Cs^+ occupied most adsorptive sites with negligible left H^+ (Fig. 7b). The decrease in peak intensity over the range of 25–40° might be due to the incorporation of Cs^+ into the structure. Hence, the adsorption capacity increased sharply at the initial concentration higher than 8250 mg/L. The q_e of 620 mg/g (4.66 mmol/g) at high Cs^+ concentrations over 8250 mg/L (62.08 mmol/L) was nearly identical to the theoretical q_e (612 mg/g or 4.60 mmol/g) calculated from the sum of all K^+ and Ca^{2+} in $K_{1.35}Ca_{0.91}Sn_3S_{7.59}$ (Fig. 2d). When the saturated adsorbent was regenerated with the K^+ solution, its capacity decreased slightly to 4.37 mmol/g (581 mg/g, Fig. 2d) at pH 2, leaving 0.29 mmol/g sites of K^+. As a result, we are convinced that in acidic solutions with extra high Cs^+ concentrations, the majority of the Ca^{2+} and K^+ contained in KCaSnS were replaced with Cs^+.

4.4. New design strategy

The radioactive Cs^+-rich wastewater with high acidity and salinity is difficult to treat with conventional adsorbents. Recently, Tang et al. [24] reported a new metal sulfide adsorbent InSnS-1 that exhibited excellent acid resistance even at pH 0. On the contrary, this study aimed to improve the adsorption efficiency at pH conditions that most adsorption studies have employed, at high acidity conditions in particular. Hence, we synthesized a layered KCaSnS incorporating metastable Ca^{2+} into the Sn-S matrix, where Ca^{2+} is large enough to reserve space for locating Cs^+ during adsorption. The structural Ca^{2+} ions were leached out in the acidic condition and their sites were replaced with Cs^+. As the structure of KCaSnS is rather stable, even partial leaching of the constituent ions requires a certain level of acidity, i.e., pH 2 in this case. Upon the release of weakly bonded Ca^{2+} ions from the crystal structure, preferential adsorption of Cs^+ would take place due to its high affinity toward S^{2-}. Because proton is a very hard Lewis acid, it may not dominate the structural Ca^{2+} empty sites. Furthermore, as previously mentioned, proton alone cannot leach off all of the structural Ca^{2+}. To increase the likelihood of Cs^+ being accessible into the structure, the structural Ca^{2+} must be completely removed. This requires very high Cs^+ concentrations, even higher than H^+ concentrations. The commencement of Cs^+ concentration of 62.08 mmol/L for the complete leaching at pH 2 indicates a synergistic interaction of Cs^+ and H^+, resulting in the maximum adsorption capacity of 4.66 mmol/g.

5. Conclusions

We have found that the coexistence of ample H^+ and Cs^+ is instrumental in completely leaching the structural Ca^{2+} from the Sn-S matrix. The adsorbent design strategy that incorporates structural lattice points into interlayer space of typical layered materials overturns our previous understanding. Notably, the Cs^+ adsorption capacity is greater in acidic solutions than that in neutral solutions, which contradicts the general trend of current SnS-type adsorbents. At first, a conspicuous increase in Cs^+ adsorption capacity in acid was not noticed, although the release of appreciable amount of the structural Ca^{2+} was observed at 500 mg/L Cs^+ and pH 2, for example. Then, we attempted a much higher concentration of Cs^+, i.e., above 8250 mg/L and could spot a steep rise in Cs^+ adsorption capacity. The structure-damaging proton is used to mediate ion exchange in this case. The uncommon ion-exchange possibility is accomplished by the synthesis of an *intermediate* metastable crystal structure that can resist transformation while permitting ion exchange. We believe that our approach provides meaningful insights for the design of different types of novel adsorbents.

Environmental implication

^{137}Cs, as a main hazardous radionuclide in acidic wastewater generated during spent fuel reprocessing and decommissioning of nuclear power plants, poses a threat to human health. However, the Cs^+ adsorption performance of most adsorbents in acidic conditions has an insurmountable limit due to the presence of copious protons. In this study, we turn the problematic proton into a functional agent by incorporating a large, weakly bonding ion, Ca^{2+} into Sn-S matrix.

Leaching Ca^{2+} from the matrix creates additional adsorption sites in potassium calcium thiostannate (KCaSnS) resulting in the greater Cs^{+} adsorption capacity in acidic solutions than that in neutral solutions.

CRediT authorship contribution statement

Chenyang Yang: Conceptualization, Investigation, Visualization, Writing – original draft. **Yong Jae Suh:** Conceptualization, Validation, Writing – review & editing. **Kuk Cho:** Conceptualization, Validation, Writing – review & editing, Supervision.

Declaration of Competing Interest

The authors declare the following financial interests/personal relationships which may be considered as potential competing interests: Kuk Cho reports financial support was provided by National Research Foundation of Korea. Yong Jae Suh reports financial support was provided by Ministry of Science and ICT of Korea.

Data Availability

Data will be made available on request.

Acknowledgements

This work was supported by the National Research Foundation (NRF) grant funded by the Ministry of Education, Republic of Korea [2020R1A6A1A03044834; 2022R1I1A3063150] and the Basic Research Project [GP2022–011, 23–3212–2] of the Korea Institute of Geoscience and Mineral Resources (KIGAM) funded by the Ministry of Science and ICT of Korea.

Appendix A. Supporting information

Supplementary data associated with this article can be found in the online version at doi:10.1016/j.jhazmat.2023.131648.

References

[1] Aguila, B., Banerjee, D., Nie, Z., Shin, Y., Ma, S., Thallapally, P.K., 2016. Selective removal of cesium and strontium using porous frameworks from high level nuclear waste. Chem Commun 52, 5940–5942. https://doi.org/10.1039/C6CC00843G.

[2] Aslanov, L., Zakharov, V., Paseshnichenko, K., Yatsenko, A., Orekhov, A., Tafeenko, V., Chernyshev, V., 2018. Design of 2D-nanocrystals in water: preparation, structure and functionalization. Pure Appl Chem 90, 833–844. https://doi.org/10.1515/pac-2017-1105.

[3] Ding, D., Cheng, L., Wang, K.-Y., Liu, H.-W., Sun, M., Wang, C., 2020. Efficient Cs^{+}–Sr^{2+} separation over a microporous silver selenidostannate synthesized in deep eutectic solvent. Inorg Chem 59, 9638–9647. https://doi.org/10.1021/acs.inorgchem.0c00770.

[4] El-Naggar, I.M., Zakaria, E.S., Ali, I.M., Khalil, M., El-Shahat, M.F., 2012. Chemical studies on polyaniline titanotungstate and its uses to reduction cesium from solutions and polluted milk. J Environ Radioact 112, 108–117. https://doi.org/10.1016/j.jenvrad.2012.05.012.

[5] Holder, C.F., Schaak, R.E., 2019. Tutorial on powder X-ray diffraction for characterizing nanoscale materials. ACS Nano 13, 7359–7365. https://doi.org/10.1021/acsnano.9b05157.

[6] Israelachvili, J.N., 2011. Intermolecular and surface forces. Academic press.

[7] Li, J., Jin, J., Zhang, T., Ma, W., Zeng, X., Sun, H., Cheng, M., Feng, M., Huang, X., 2021. Rapid and selective uptake of Cs^{+} and Sr^{2+} ions by a layered thiostannate with acid–base and irradiation resistances. ACS EST Water 1, 2440–2449. https://doi.org/10.1021/acsestwater.1c00290.

[8] Lide, D.R., 2005. CRC handbook of chemistry and physics, internet version 2005. CRC Press, Boca Raton, FL.

[9] Ling, C., Li, X., Zhang, Z., Liu, F., Deng, Y., Zhang, X., Li, A., He, L., Xing, B., 2016. High adsorption of sulfamethoxazole by an amine-modified polystyrene–divinylbenzene resin and its mechanistic insight. Environ Sci Technol 50, 10015–10023. https://doi.org/10.1021/acs.est.6b02846.

[10] Manos, M.J., Kanatzidis, M.G., 2009. Highly efficient and rapid Cs^{+} uptake by the layered metal sulfide $K_{2x}Mn_xSn_{3-x}S_6$ (KMS-1). J Am Chem Soc 131, 6599–6607. https://doi.org/10.1021/ja900977p.

[11] Mertz, J.L., Fard, Z.H., Malliakas, C.D., Manos, M.J., Kanatzidis, M.G., 2013. Selective removal of Cs^{+}, Sr^{2+}, and Ni^{2+} by $K_{2x}Mg_xSn_{3-x}S_6$ (x = 0.5–1) (KMS-2) relevant to nuclear waste remediation. Chem Mater 25, 2116–2127. https://doi.org/10.1021/cm400699r.

[12] Moon, J., Kim, S., Choi, W., Choi, B., Chung, D., Seo, B., 2019. The status and prospect of decommissioning technology development at KAERI. J Nucl Fuel Cycle Waste Technol 17, 139–165. https://doi.org/10.7733/jnfcwt.2019.17.2.139.

[13] Moulder, J.F., Stickle, W.F., Sobol, W.M., Bomben, K.D., 1992. Handbook of x-ray photoelectron spectroscopy. Perkin-Elmer Corp.

[14] Mu, W., Chen, B., Yu, Q., Li, X., Wei, H., Yang, Y., Peng, S., 2021. A novel zirconium phosphonate adsorbent for highly efficient radioactive cesium removal. J Mol Liq 326, 115307. https://doi.org/10.1016/j.molliq.2021.115307.

[15] Nagasaki, S., Nakayama, S., 2015. Radioactive waste engineering and management. Springer.

[16] Park, Y., Lee, Y.-C., Shin, W.S., Choi, S.-J., 2010. Removal of cobalt, strontium and cesium from radioactive laundry wastewater by ammonium molybdophosphate–polyacrylonitrile (AMP–PAN). Chem Eng J 162, 685–695. https://doi.org/10.1016/j.cej.2010.06.026.

[17] Pearson, R.G., 1988. Absolute electronegativity and hardness: application to inorganic chemistry. Inorg Chem 27, 734–740. https://doi.org/10.1021/ic00277a030.

[18] Rathore, E., Pal, P., Biswas, K., 2017. Reversible and efficient sequestration of cesium from water by the layered metal thiophosphate $K_{0.48}Mn_{0.76}PS_3{\cdot}H_2O$. Chem – A Eur J 23, 11085–11092. https://doi.org/10.1002/chem.201701883.

[19] Sarma, D., Malliakas, C.D., Subrahmanyam, K.S., Islam, S.M., Kanatzidis, M.G., 2016. $K_{2x}Sn_{4-x}S_{8-x}$ (x = 0.65–1): a new metal sulfide for rapid and selective removal of Cs^{+}, Sr^{2+} and UO_2^{2+} ions. Chem Sci 7, 1121–1132. https://doi.org/10.1039/C5SC03040D.

[20] Shannon, R.D., 1976. Revised effective ionic radii and systematic studies of interatomic distances in halides and chalcogenides. Acta Crystallogr Sect A: Cryst Phys, Diffr, Theor Gen Crystallogr 32, 751–767. https://doi.org/10.1107/S0567739476001551.

[21] Sochacki, A., Yadav, A.K., Srivastava, P., Kumar, N., Fitch, M.W., Mohanty, A., 2018. Constructed wetlands for metals: removal mechanism and analytical challenges. Constr Wetl Ind Wastewater Treat 223–247.

[22] Sugiura, Y., Makita, Y., Horie, M., 2021. Ammonium-to-sodium ion-exchange process at the interlayer of octacalcium phosphate. RSC Adv 11, 39503–39507. https://doi.org/10.1039/D1RA07939E.

[23] Suh, Y.J., Chae, J.W., Jang, H.D., Cho, K., 2015. Role of chemical hardness in the adsorption of hexavalent chromium species onto metal oxide nanoparticles. Chem Eng J 273, 401–405. https://doi.org/10.1016/j.cej.2015.03.095.

[24] Tang, J.-H., Jin, J.-C., Li, W.-A., Zeng, X., Ma, W., Li, J.-L., Lv, T.-T., Peng, Y.-C., Feng, M.-L., Huang, X.-Y., 2022. Highly selective cesium(I) capture under acidic conditions by a layered sulfide. Nat Commun 13, 658. https://doi.org/10.1038/s41467-022-28217-8.

[25] Valsala, T.P., Sonavane, M.S., Kore, S.G., Sonar, N.L., De, V., Raghavendra, Y., Chattopadyaya, S., Dani, U., Kulkarni, Y., Changrani, R.D., 2011. Treatment of low level radioactive liquid waste containing appreciable concentration of TBP degraded products. J Hazard Mater 196, 22–28.

[26] Wang, L., Pei, H., Sarma, D., Zhang, X.-M., MacRenaris, K., Malliakas, C.D., Kanatzidis, M.G., 2019. Highly selective radioactive $^{137}Cs^{+}$ capture in an open-framework oxysulfide based on supertetrahedral cluster. Chem Mater 31, 1628–1634. https://doi.org/10.1021/acs.chemmater.8b04877.

[27] Wang, R., Chen, H., Xiao, Y., Hadar, I., Bu, K., Zhang, X., Pan, J., Gu, Y., Guo, Z., Huang, F., Kanatzidis, M.G., 2019. $K_x[Bi_{4-x}Mn_xS_6]$, design of a highly selective ion exchange material and direct gap 2D semiconductor. J Am Chem Soc 141, 16903–16914. https://doi.org/10.1021/jacs.9b08674.

[28] Whittles, T.J., 2018. Electronic Characterisation of Earth-Abundant Sulphides for Solar Photovoltaics. Springer.

[29] Yang, C., Cho, K., 2021. Rapid and selective removal of Cs^{+} from water by layered potassium antimony thiostannate. J Hazard Mater 403, 124105. https://doi.org/10.1016/j.jhazmat.2020.124105.

[30] Yang, C., Suh, Y.J., Cho, K., 2022. Highly selective cesium removal under acidic and alkaline conditions using a novel potassium aluminum thiostannate. Chemosphere 301, 134610. https://doi.org/10.1016/j.chemosphere.2022.134610.

[31] Yang, H.-M., Park, C.W., Kim, I., Yoon, I.-H., 2020. Hollow flower-like titanium ferrocyanide structure for the highly efficient removal of radioactive cesium from water. Chem Eng J 392, 123713. https://doi.org/10.1016/j.cej.2019.123713.

[32] Zhang, H., Li, C., Chen, X., Fu, H., Chen, Y., Ning, S., Fujita, T., Wei, Y., Wang, X., 2022. Layered ammonium vanadate nanobelt as efficient adsorbents for removal of Sr^{2+} and Cs^{+} from contaminated water. J Colloid Interface Sci 615, 110–123. https://doi.org/10.1016/j.jcis.2022.01.164.

[33] Zhao, Y.-M., Cheng, L., Wang, K.-Y., Hao, X., Wang, J., Zhu, J.-Y., Sun, M., Wang, C., 2022. pH-controlled switch over coadsorption and separation for mixed Cs^{+} and Sr^{2+} by an acid-resistant potassium thioantimonate. Adv Funct Mater 32, 2112717. https://doi.org/10.1002/adfm.202112717.

[34] Zou, Y.-M., Ma, W., Sun, H.-Y., Tang, J.-H., Lv, T.-T., Feng, M.-L., Huang, X.-Y., 2022. High-capacity recovery of Cs^{+} ions by facilely synthesized layered vanadyl oxalatophosphates with the clear insight into remediation mechanism. J Hazard Mater 434, 128869. https://doi.org/10.1016/j.jhazmat.2022.128869.